Volume 23, No 2 | International Journal of Radiation Research, April 2025

Clinical efficacy of albumin-bound paclitaxel combined with carboplatin in the treatment of nasopharyngeal carcinoma

M. Huang*, G. Wang, F. Xuan

Department of Radiotherapy, Zhuji People's Hospital, Zhuji 311809, Zhejiang Province, China

► ***Original article***

Corresponding author:
Minguang Huang, M.D.,
E-mail: *jiqawrp975@163.com*

Received: August 2024
Final revised: November 2024
Accepted: November 2024

Int. J. Radiat. Res., April 2025; 23(2): 427-433

DOI: 10.61186/ijrr.23.2.23

Keywords: *Albumin-bound paclitaxel, carboplatin, nasopharyngeal carcinoma; dynamic contrast-enhanced MRI, serum biomarkers, clinical efficacy.*

ABSTRACT

Background: This study aims to evaluate the clinical efficacy of concurrent chemoradiotherapy for nasopharyngeal carcinoma (NPC) following induction chemotherapy (IC) with albumin-bound paclitaxel (ABP) combined with carboplatin, through the analysis of serum biomarkers and dynamic contrast-enhanced magnetic resonance imaging (MRI) data. ***Material and Methods:*** Ninety-six NPC patients were rolled into Group I (concurrent chemoradiotherapy) and Group II (IC with ABP and carboplatin+concurrent chemoradiotherapy). DCE-MRI scans were utilized to evaluate changes in lesion characteristics. Serum samples were collected to analyze tumor markers including cytokeratin 19 fragment antigen 21-1 (CYFRA21-1), SCC-associated antigen (SCC-Ag), and carbohydrate antigen 125 (CA-125), as well as superoxide dismutase (SOD), glutathione peroxidase (GSH-Px) activity, and malondialdehyde (MDA) levels. Toxicities and 2-year overall survival (OS) and progression-free survival (PFS) were also assessed. ***Results:*** Group II exhibited a markedly higher objective response rate and disease control rate versus Group I (35.4% vs. 58.3%, 50.0% vs. 81.3%, respectively). MRI scans revealed a drastic reduction in the proportion of patients with obvious enhancement of primary lesions, invasion of the base of the skull/medial pterygoid muscle, etc. Serum levels of CYFRA21-1, SCC-Ag, CA125, and MDA were greatly decreased, while SOD and GSH-Px activities were notably increased ($P<0.05$). Group II showed a considerable increase in OS and PFS versus Group I (75.0% vs. 89.6%, 68.8% vs. 83.3%, respectively, $P<0.05$). ***Conclusion:*** the combination of ABP and carboplatin has demonstrated enhanced efficacy and improved survival outcomes in patients with NPC, providing new insights and evidence for clinical application.

INTRODUCTION

Nasopharyngeal carcinoma (NPC) arises from the metaplastic columnar epithelium in the nasopharyngeal region, commonly found in the lateral walls and posterosuperior wall. Its incidence has been increasing annually [1, 2]. Due to its unique anatomical location, often surrounded by a rich vascular network and numerous critical organs, the diagnosis and treatment of NPC pose significant challenges. Concurrent chemoradiotherapy is the preferred therapeutic modality for NPC [3]. However, because NPC typically presents with an insidious onset and early symptoms are often subtle, many patients are diagnosed at a locally advanced stage, frequently accompanied by invasion of the adjacent skull base and cervical lymph node metastasis [4]. Consequently, the five-year overall survival (OS) rate after chemoradiotherapy alone remains low [5]. Tumor sensitivity to chemoradiotherapy is a crucial factor affecting treatment outcomes and prognosis. Therefore, enhancing the clinical efficacy for patients with locally advanced NPC is a key focus of current research.

Clinically, concurrent chemoradiotherapy is commonly used for the treatment of NPC. Radiotherapy can disrupt the normal structure of tumor cells through radiation, increase the uptake of chemotherapeutic drugs into the cells, and enhance cytotoxic effects [6]. Paclitaxel, a taxane chemotherapeutic agent, and albumin-bound paclitaxel (ABP), a novel formulation using nanotechnology to encapsulate paclitaxel in albumin, have shown improved therapeutic efficacy and reduced adverse reactions [7]. Platinum-based chemotherapeutic agents can inhibit DNA synthesis in tumor cells and interfere with their proliferation, growth, and migration. Clinically, ABP combined with carboplatin is widely used in the treatment of various cancers [8-10]. Previous studies demonstrated that concurrent chemoradiotherapy following induction chemotherapy (IC) is highly effective in treating NPC, reducing distant metastasis and recurrence rates, and improving patient survival [11]. Dynamic contrast-enhanced magnetic resonance imaging (DCE-MRI) can reflect the perfusion status of target tissues and indirectly assess hypoxia and ischemia, making it useful for evaluating the efficacy of chemoradiotherapy in NPC [12]. However, research on the use of ABP combined with carboplatin in IC for

[Downloaded from mail.ijrr.com on 2025-12-22]

[DOI: 10.61186/ijrr.23.2.23]

NPC is relatively limited.

The Aim of this work was to assess clinical efficacy of DCE-MRI in assessing the response of NPC to IC with ABP and carboplatin followed by concurrent chemoradiotherapy. Additionally, we analyzed the changes in serum tumor markers, as well as the treatment-related toxicities and long-term outcomes. This study is the first to systematically evaluate the clinical efficacy of concurrent chemoradiotherapy for NPC following IC with ABP combined with carboplatin, through a comprehensive analysis of serum biomarkers and DCE-MRI data. This study analyzed the impact of this treatment regimen relative to traditional concurrent chemoradiotherapy (CCRT) on objective response rate (ORR), disease control rate (DCR), two-year OS, and progression-free survival (PFS) in patients with NPC. The study revealed the positive effects of this regimen in reducing enhancement of primary lesions, the ratio of invasion to the skull base/internal pterygoid muscle, and improving antioxidant capacity, providing new evidence and clinical insights for the treatment of NPC and addressing gaps in the efficacy and survival outcomes of existing treatment protocols.

MATERIALS AND METHODS

Case information

Ninety-six patients diagnosed with NPC and treated at Zhuji People's Hospital from June 2021 to June 2022 were recruited. Inclusion criteria: (1) meeting the *American Joint Committee on Cancer/ International Union Against Cancer* diagnostic criteria for NPC and confirmed by pathological examination; (2) receiving initial treatment; (3) expected survival of more than 6 months; (4) having indications for chemotherapy; (5) Karnofsky performance status (KPS) score >70. Exclusion criteria: (1) concomitant malignant tumors in other sites; (2) concomitant significant organ dysfunction of the heart, liver, or kidneys; (3) mental abnormalities or inability to cooperate with treatment; (4) allergy to the drugs used in this study; (5) inability to tolerate chemotherapy.

The 96 patients were enrolled into Group I and II based on the treatment methodologies, with 48 patients in each group. The clinical treatment statistics for both groups of patients are shown in Table 1, with neglectable differences observed in age, gender, tumor stage, tumor type, or KPS scores between the two groups (P>0.05). All participants signed informed consent forms. The Institutional Review Board of Zhuji People's Hospital approved this work (Approval number: 2022-1112, Registration date: 2022.11.12).

Therapeutic methodologies

Patients in Group I received concurrent chemoradiotherapy. Head-neck-shoulder thermo-plastic mask (Guangzhou Renfu Medical Equipment Co., Ltd., Guangzhou, Guangdong Province, China) was employed for immobilization of patients in supine position. A 16-row large-aperture helical CT simulator, Brilliance™ Big Bore CT (Philips, Amsterdam, Netherlands), was employed to scan the range from head top to 3 cm below the clavicle. Subsequently, the target areas were localized (the non-metastatic cervical lymphatic drainage area was considered the low-risk area; the primary lesion and its surrounding area, as well as the metastatic cervical lymphatic drainage area, were considered high-risk areas; the tumor area was defined as the region within 3-5 mm around the primary lesion and metastatic lymph nodes), at 50-55 Gy/28-30 fractions delivered to the low-risk area, 60-65 Gy/30-33 fractions to the high-risk area, and 68 Gy/33 fractions to the tumor area, administered 4-5 times per week, with a total treatment duration of 6 weeks (a total of 33 treatment sessions). Intravenous infusion of 40 mg/m^2 of carboplatin (Approval No.: National Medical Products Administration Approval Number H20020180; Specification: 100 mg; Manufacturer: Qilu Pharmaceutical Co., Ltd., Jinan, Shandong Province, China) was administered once per week.

Table 1. Clinical data statistics of two patient groups.

Group	Case number	Age (years old)	Sex		Tumor stage		Tumor type		KPS score
			Male	Female	III	IV	Squamous cell carcinoma	Undifferentiated carcinoma	
Group I	48	57.1±4.8	30	18	31	17	33	15	75.4±3.3
Group II	48	58.5±4.4	31	17	28	20	31	17	76.0±4.5
P		0.498	0.788		0.604		0.752		0.380

KPS: Karnofsky performance status.

Patients in Group II received concurrent chemoradiotherapy following IC with ABP and carboplatin. Intravenous infusion of 135 mg/m^2 of ABP (Approval No.: National Medical Products Administration Approval Number H20183378; Specification: 100 mg; Manufacturer: Jiangsu Hengrui Medicine Co., Ltd., Lianyungang, Jiangsu Province, China) combined with 80 mg/m^2 of carboplatin (day 1) was administered every 3 weeks, with each cycle lasting for 21 days. Two cycles of chemotherapy were administered. Concurrent chemoradiotherapy was initiated 21 days after the completion of IC.

Observation indicators

MRI scan: Patients underwent scanning with the Signa HD 1.5T superconducting MRI system (GE Healthcare, Fairfield, Connecticut, USA) both before treatment and three months post-treatment. Prior to

[Downloaded from mail.ijrr.com on 2025-12-22]

[DOI: 10.61186/ijrr.23.2.23]

scanning, routine venipuncture was performed. A head-neck coil was utilized for routine and contrast-enhanced MRI of the skull base, nasopharynx, and neck while the patients were positioned supine. Routine transverse scans of the nasopharynx were performed with T2-weighted imaging (T2WI) parameters set at TR (repetition time)=4,780 ms and TE (echo time)=88.5 ms, and T1WI parameters set at TR=360 ms and TE=13.5 ms. Routine coronal scans of the nasopharynx were performed with parameters set at TR=520 ms and TE=8.5 ms. After the routine scanning, 0.1 mmol/kg of Gd-DTPA contrast agent (Shanghai BRACCO SINE Pharmaceutical Co., Ltd., China) was injected through the elbow venous puncture channel, followed by contrast-enhanced scanning. Transverse T1WI: TR=320 ms and TE=2.5 ms, coronal scanning: TR=255 ms and TE=1.5 ms, and sagittal scanning parameters were set at TR=305 ms and TE=2.3 ms. The above scans were all conducted using the chemical saturation fat suppression sequence, and the following parameters were added: field of view=240 mm, slice thickness=4 mm, spacing=1 mm, number of excitations=2. After the scan images were uploaded to the workstation, the lesion size, enhancement degree, and the extent of invasion to the surrounding area were examined at the same level, window position, and window width.

Efficacy evaluation: Before treatment and at three months post-treatment, nasopharyngeal fiberoptic endoscopy and MRI examinations were conducted, and the treatment efficacy was assessed regarding *Response Evaluation Criteria in Solid Tumors version 1.1* [13] as follows: (1) complete remission (CR); (2) partial remission (PR); (3) stable disease (SD); (4) progressive disease (PD). ORR=(CR+PR)/total×100%. DCR=(CR+PR+SD)/total×100%.

Detection of serum tumor markers: Pre-treatment (0w) and at the end of 6 weeks of treatment (6w), 3 mL of fasting elbow venous blood samples were collected. Cytokeratin 19 fragment antigen 21-1 (CYFRA21-1) and SCC-associated antigen (SCC-Ag) were measured using the enzyme-linked immunosorbent assay (ELISA). Both the CYFRA21-1 and SCC-Ag kits were obtained from CanAg Diagnostics, Sweden. The diluted standards and sample diluents were added to the wells of the microplate, followed by the addition of enzyme conjugates. The plates were incubated at 37°C for 1 hour. After washing, one drop of substrate solution was applied to each well, and the plates were kept in the dark for 10 minutes. The reaction was then terminated by adding stop solution, and the optical density of each well was measured within 5 minutes at a wavelength of 450 nm using a microplate reader (Wellscan MK3, Rebus, Finland).

Carbohydrate antigen 125 (CA-125) was measured using a chemiluminescent method, strictly following the instructions provided in the kit (Biosystems, Tianjin, China). The analysis was performed using the Abbott AXSYM system, an automated chemiluminescent immunoassay analyzer (Abbott Laboratories, USA).

Detection of serum oxidative stress indicators: Superoxide dismutase (SOD), glutathione peroxidase (GSH-Px) activity, and malondialdehyde (MDA) in the serum were measured using ELISA kits (Solarbio Technology Co., Ltd., Beijing, China).

Evaluation of toxic side effects: Regarding *Common Terminology Criteria for Adverse Events 3.0* standard [14], the severity of common adverse events during the treatment process was evaluated on a scale ranging from grade 0 to grade IV.

Follow-up: After the completion of treatment, follow-up assessments were conducted every three months for a period of two years. Follow-up methods included telephone calls, online platforms, and outpatient visits. The follow-up evaluations encompassed complete blood counts, serum tumor marker assessments, liver and kidney function tests, and MRI scans of the head and neck. All patients were followed up until March 2024, with no cases lost to follow-up in either group.

Statistical methodologies

Employing *SPSS 24.0*, categorical data (%) were analyzed by χ^2 test. Continuous data (mean±SD) were analyzed by Student's t-test. Kaplan-Meier curves were plotted to calculate OS and PFS, and the log-rank test was adopted. Differences were statistically significant when $P<0.05$.

RESULTS

Efficacy

The difference in clinical efficacy of patients is illustrated in figure 1. In Group I, there were 2 cases of CR (4.2%), 15 cases of PR (31.3%), 7 cases of SD (14.6%), and 24 cases of PD (50.0%). After calculation, the ORR was found to be 35.4%, and the DCR was 50.0%. In Group II, there were 8 cases of CR (16.7%), 20 cases of PR (41.7%), 11 cases of SD (22.9%), and 9 cases of PD (18.8%). After calculation, the ORR was found to be 58.3%, and the DCR was 81.3%. Both the ORR and DCR in Group II were relatively higher ($P<0.05$).

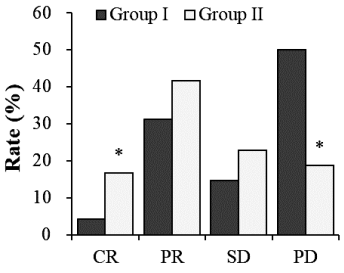

Figure 1. Comparison of clinical efficacy in NPC patients.
** meant P<0.05 vs. Group I*

[Downloaded from mail.ijrr.com on 2025-12-22]

[DOI: 10.61186/ijrr.23.2.23]

Comparison of two sets of MRI enhanced scanning features

MRI images revealed thickening of the soft tissues of the posterior nasopharyngeal wall in a patient with nasopharyngeal carcinoma. The tissue showed isointensity on T1WI and hyperintensity on T2WI, with more pronounced thickening on the left side. Nasopharyngeal recess narrowing was observed, while the bilateral longus capitis and pterygoid muscles appeared normal in both morphology and signal intensity. There was no evidence of bone destruction in the bilateral skull base, and multiple small lymph nodes are noted within the submandibular, parapharyngeal, and carotid sheath spaces. Bilateral maxillary and ethmoidal sinus mucosal thickening were present, as well as symmetric hypertrophy of the inferior turbinates. No abnormal signals were seen in the cervical spine, and no enhancement was noted post-contrast administration. Gd-DTPA enhanced imaging demonstrated marked and relatively homogeneous enhancement of the nasopharyngeal lesion (figure 2).

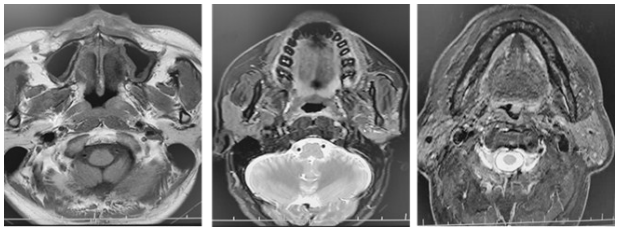

Figure 2. MRI images of a NPC patient. (Male, 48 years old, with a nasopharyngeal mass).

Comparison of MRI enhancement scan characteristics between groups is presented in table 2. Following treatment, the proportions of obvious enhancement primary lesions, invasion pharynx side clearance/oropharyngeal, invasion base of skull/ medial pterygoid muscle, invasion cranial nerves/ cavernous sinus/sinuses/limb muscles, and enlargement of lymph node in neck and retropharyneal node were greatly lower in both Group I and Group II relative to pre-treatment (P<0.05). Additionally, following treatment, proportions of obvious enhancement primary lesions, invasion base of skull/medial pterygoid muscle, invasion cranial nerves/cavernous sinus/ sinuses/limb muscles, and enlargement of lymph node in neck and retropharyneal node were markedly lower in Group II (P<0.05).

Serum tumor markers

Comparison of the changes in serum tumor markers CYFAR21-1, SCC-Ag, and CA125 levels before and after treatment between groups is shown in figure 3. CYFRA21-1, SCC-Ag, and CA-125 levels differed slightly between the two groups of patients at baseline (0w) (P>0.05). At 6 weeks post-treatment, the levels for Group I were (6.73±1.51) μg/L for CYFRA21-1, (4.04±0.64) ng/mL for SCC-Ag, and (44.25±6.63) kU/L for CA-125. In comparison, Group II showed levels of (4.08±1.66) μg/L for CYFRA21-1, (2.33±0.45) ng/mL for SCC-Ag, and (28.19±5.24) kU/ L for CA-125. Following treatment, serum levels of CYFAR21-1, SCC-Ag, and CA125 in both Group I and Group II patients were substantially inferior to pre-treatment (P<0.05). Moreover, post-treatment, CYFAR21-1, SCC-Ag, and CA125 in Group II patients were markedly inferior to those in Group I (P<0.05).

Table 2. Analysis of MRI enhanced scanning features in NPC patients.

Features	Group I (n=48)		Group II (n=48)	
	0w	6w	0w	6w
Obvious enhancement primary lesions	48 (100.0)	13 (27.1)①	48 (100.0)	5 (10.4)①②
Invasion pharynx side clearance/oropharyngeal	9 (18.8)	1 (2.1)①	10 (20.8)	0 (0.0)①
Invasion base of skull/medial pterygoid muscle	28 (58.3)	7 (14.6)①	30 (62.5)	3 (6.3)①②
Invasion cranial nerves/ cavernous sinus/sinuses/limb muscles	12 (25.0)	5 (10.4)①	11 (22.9)	1 (2.1)①②
Enlargement of lymph node in neck and retropharyneal node	40 (83.3)	11 (22.9)①	41 (85.4)	3 (6.3)①②

Note: ①P<0.05 vs. pre-treatment, ②P<0.05 vs. Group I (also in figures).

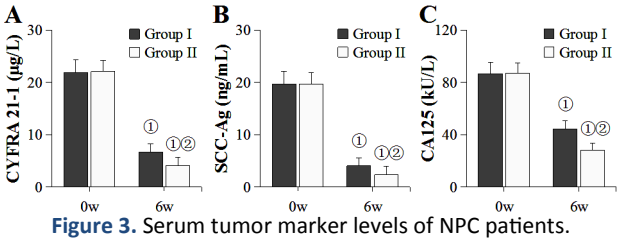

Figure 3. Serum tumor marker levels of NPC patients.
Note: **(A)** Serum CYFAR21-1 level; **(B)** Serum SCC-Ag levels; **(C)** Serum CA125 level.
①*P<0.05 vs. pre-treatment,* ②*P<0.05 vs. Group I*

Oxidative stress indicators between two groups

Comparison of the changes in serum oxidative stress markers before and after treatment between groups is illustrated in figure 4. SOD, GSH-Px, and MDA levels differed slightly between the two groups of patients at baseline (0w) (P>0.05). At 6 weeks post -treatment, Group I exhibited levels of (55.61±4.24) U/mL for SOD, (61.89±5.34) AU for GSH-Px, and (13.13±1.11) mmol/L for MDA. In contrast, Group II had levels of (65.07±4.11) U/mL for SOD, (80.36±6.09) AU for GSH-Px, and (11.15±1.38) mmol/ L for MDA. Following treatment, SOD, GSH-Px, and MDA in both Group I and Group II patients were considerably superior to before treatment (P<0.05). Furthermore, post-treatment, SOD and GSH-Px in Group II patients were notably superior to those in Group I, while the MDA level was greatly inferior to in Group I (P<0.05).

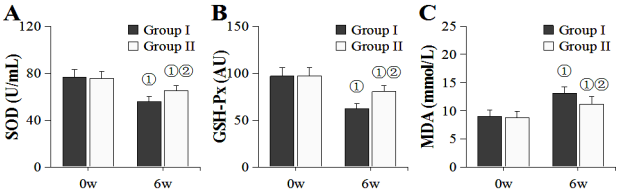

Figure 4. Serum oxidative stress levels of NPC patients.

[Downloaded from mail.ijrr.com on 2025-12-22]

[DOI: 10.61186/ijrr.23.2.23]

Two sets of toxic side effects

Figure 5 illustrates the comparison of adverse event grading during treatment between the groups. The common adverse events observed in both patient groups included leukopenia, thrombocytopenia, liver and kidney injury, dermatitis, mucosal reactions, gastrointestinal reactions, and myelosuppression. The proportions of adverse events graded from 0 to IV differed slightly between the two groups (P>0.05) across different adverse events.

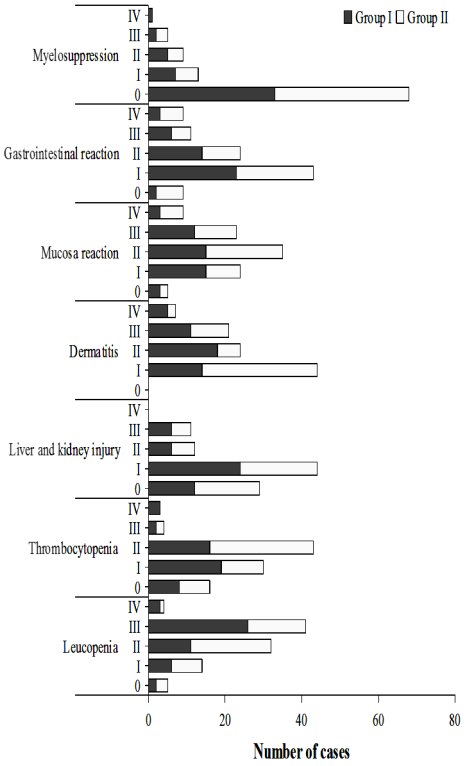

Figure 5. Comparison of toxicity and side effects grading in NPC patients.

Long-term therapeutic effects

From the Kaplan-Meier curves shown in figure 6, it was found that the OS for Group I was 75.0%, and the PFS was 68.8%; while for Group II, OS was 89.6%, and PFS was 83.3%. OS and PFS of Group II patients were greatly superior to those of Group I (P<0.05).

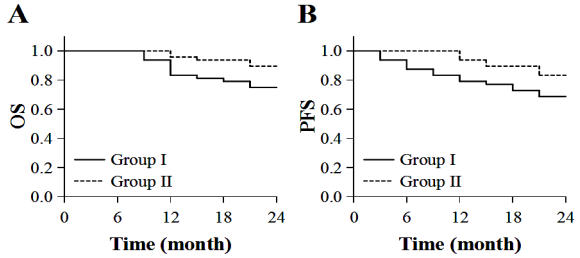

Figure 6. Long term efficacy comparison of NPC patients. Note: **(A)** OS; **(B)** PFS.

DISCUSSION

The nasopharynx serves as a bridge between the oral cavity, pharynx, and nasal cavity, playing a vital role in the respiratory pathway. However, influenced by factors such as viral infections, genetics, and the environment, the incidence of NPC has been gradually increasing [15]. The etiology of NPC remains unclear, and its anatomical location is both concealed and distinctive. Without active intervention and treatment measures, NPC can lead to distant metastasis, thereby impacting the patients' overall health and survival. NPC exhibits a relatively high sensitivity to radiotherapy and chemotherapy, which stands as the primary modality for advanced NPC, significantly improving patient prognosis [16, 17]. Concurrent chemoradiotherapy is a standard treatment approach for NPC. However, due to its limited treatment window, if tumor cells exhibit low sensitivity to concurrent chemoradiotherapy, additional therapeutic interventions may be necessary. Currently, the clinical induction regimens for NPC are not standardized and are often chosen based on their mechanisms of action and resistance mechanisms for combination therapy with two or more agents, such as paclitaxel plus cisplatin, paclitaxel plus carboplatin, and 5-fluorouracil plus cisplatin [18-20]. Paclitaxel can promote microtubule assembly, inhibit microtubule depolymerization and cell mitosis, affecting tumor cell division, exerting anticancer effects [21]. Compared to solvent-based paclitaxel, ABP assembled using nanotechnology does not require a co-solvent, thus increasing drug dosage intensity and reducing adverse reactions. Multiple studies confirmed that the complete remission rate or survival rate of clinical cell carcinoma of the head and neck treated with ABP is significantly higher than that of docetaxel [22, 23]. This work assessed the clinical efficacy of ABP combined with carboplatin IC followed by synchronous radiotherapy and chemotherapy in treating NPC, aiming to provide reference for finding a more suitable treatment approach.

MRI technology offers high resolution for soft tissue imaging, allowing for precise localization, orientation, and evaluation of surrounding tissue changes in tumors. With the rapid development of MRI technology, dynamic contrast-enhanced MRI scans can provide insights into the hemodynamic changes within tumor tissues using contrast agents. The degree of early enhancement in tumors can reflect the level of vascularity and tissue perfusion. Early enhancement increases with the elevation of tumor tissue blood flow perfusion levels [24]. This study utilized DCE-MRI scans to assess changes in tumor status in NPC patients before and after treatment. The results revealed a significant decrease in the proportion of marked enhancement in primary lesions, invasion of the base of the skull/medial pterygoid muscle, invasion of cranial nerves/ cavernous sinus/sinuses/limb muscles, and enlargement of lymph nodes in the neck and retropharyngeal regions following treatment. DCE-MRI involves the intravenous administration of contrast agents, which enter the tumor

[Downloaded from mail.ijrr.com on 2025-12-22]
[DOI: 10.61186/ijrr.23.2.23]

microvasculature via the bloodstream. This technique allows for the assessment of changes in tumor vascular permeability, providing crucial information for early treatment evaluation and overall outcome prediction [25]. In addition to imaging examinations, serum tumor markers can also be used for early cancer screening, treatment evaluation, and prediction [26]. Tumor cells in the body can activate proteases and promote cell degradation, leading to the release of CYFRA21-1 into the bloodstream, resulting in elevated peripheral blood CYFRA21-1 levels in patients [27]. SCC-Ag belongs to the glycoprotein-related antigen family of serine protease inhibitors and is primarily present in the cytoplasm of squamous epithelial cell carcinomas [28]. CA125 is a mucin-like glycoprotein with high diagnostic sensitivity for common tumors [29]. This study found CYFRA21-1, SCC-Ag, and CA125 in NPC patients decreased after treatment with different regimens, and were lower in patients treated with ABP combined with carboplatin IC followed by synchronous radiotherapy and chemotherapy. This indicates that IC combined with synchronous radiotherapy and chemotherapy can exacerbate the degree of structural damage to tumor cells, interfere with DNA synthesis in tumor cells, suppress abnormal expression of epidermal growth factor receptors, and subsequently reduce tumor marker levels in the serum.

The progression of NPC is associated with inflammatory responses. After synchronous radiotherapy and chemotherapy, leading to the exacerbation of oxidative stress responses and resulting in cell apoptosis [30]. SOD is a crucial antioxidant enzyme in the body, which catalyzes the conversion of O_2^- to H_2O_2 and O_2, and thus can be used to assess the degree of oxidative stress within cells [31]. GSH-Px catalyzes the reduction of glutathione to H_2O_2, maintaining the intracellular status of glutathione, thereby protecting cells from oxidative stress damage [32]. When oxygen free radicals interact with lipids and undergo oxidation reactions, the final product of this oxidation is MDA, which serves as an indicator of the degree of membrane lipid peroxidation [33]. This study found that the activities of SOD and GSH-Px in peripheral blood decreased, while MDA levels increased in NPC patients following treatment with various regimens. However, in patients treated with ABP combined with carboplatin IC followed by synchronous radiotherapy and chemotherapy, the activities of SOD and GSH-Px were elevated, and MDA levels were reduced. This indicates that IC combined with synchronous radiotherapy and chemotherapy can selectively increase the sensitivity of tumor cells to treatment, induce compensatory release of antioxidant substances (SOD and GSH-Px activities) from normal cells, and alleviate oxidative stress damage.

Adjuvant chemotherapy can enhance the local control rate and OS rate of the disease by killing residual tumor cells locally. However, the toxic side effects of synchronous radiotherapy and chemotherapy are significant, and the tolerance and compliance of adjuvant chemotherapy are poor. Therefore, only 60-70% of patients can tolerate 2-3 cycles, with no significant improvement in patient survival rates [34]. This study found that NPC patients treated with different regimens all experienced varying degrees of toxic side effects, including leukopenia, thrombocytopenia, liver and kidney injury, dermatitis, mucosal reaction, gastrointestinal reaction, and myelosuppression. However, in patients treated with ABP combined with carboplatin IC followed by synchronous radiotherapy and chemotherapy, OS and PFS were higher. This indicates that IC combined with synchronous radiotherapy and chemotherapy can greatly prolong the survival period of NPC patients and is highly safe.

CONCLUSION

This study aimed to evaluate the clinical efficacy of concurrent chemoradiotherapy for NPC following IC with ABP combined with carboplatin, through the assessment of serum biomarkers and DCE-MRI. The results indicated that the ABP and carboplatin IC followed by concurrent chemoradiotherapy not only greatly improved the ORR and DCR but also enhanced tumor characteristics, reduces tumor marker levels, boosts antioxidant capacity, and markedly increases OS and PFS in patients. These findings suggest that the ABP and carboplatin IC regimen significantly enhances treatment outcomes and survival prognosis for NPC, providing important references for the development of treatment protocols.

ACKNOWLEDGEMENTS

Not applicable.

***Ethics approval and consent to participate*:** All participants signed informed consent forms. The Institutional Review Board of Zhuji People's Hospital approved this work (Approval number: 2022-1112, Registration date: 2022.11.12).

***Conflicts of interests*:** No conflict of interest exits in this manuscript.

***Consent for publication*:** Manuscript is approved by all authors for publication.

***Funding*:** Not applicable.

***Availability of data and materials*:** The data and materials of this experiment are available.

***Author contributions*:** G.W. were responsible for conception and design. M.H. was responsible for manuscript writing. F.X. were responsible for collection and assembly of data. M.H. and G.W. were

[Downloaded from mail.ijrr.com on 2025-12-22]

[DOI: 10.61186/ijrr.23.2.23]

responsible for data analysis and interpretation. All authors were responsible for manuscript writing. All authors were responsible for the final approval of the manuscript.

REFERENCES

1. Lee AWM, Ng WT, Chan JYW, *et al.* (2019) Management of locally recurrent nasopharyngeal carcinoma. *Cancer Treat Rev,* ***79****: 101890*. DOI: 10.1016/j.ctrv.2019.101890
2. Juarez-Vignon Whaley JJ, Afkhami M, Onyshchenko M, *et al*. (2023) Recurrent/metastatic nasopharyngeal carcinoma treatment from present to future: where are we and where are we heading? *Curr Treat Options Oncol,* ***24****(9): 1138-1166*. DOI: 10.1007/s11864-023-01101-3
3. Nazeer F, Poulose JV, Kainickal CT (2022) Induction chemotherapy in nasopharyngeal carcinoma - A systematic review of phase III clinical trials. *Cancer Treat Res Commun,* ***32****: 100589*. DOI: 10.1016/j.ctarc.2022.100589
4. Fan Y, Hui M, Li F, *et al*. (2024) Establishment of nomogram prediction model for distant metastasis of nasopharyngeal carcinoma after radiotherapy. *Int J Radiat Res,* ***22****(2): 373-378*. DOI: 10.61186/ijrr.22.2.373
5. You R, Liu Y-P, Huang P-Y, *et al*. (2020) Efficacy and safety of locoregional radiotherapy with chemotherapy vs chemotherapy alone in de novo metastatic nasopharyngeal carcinoma: A multicenter phase 3 randomized clinical trial. *JAMA Oncol,* ***6****(9): 1345-1352*. DOI: 10.1001/jamaoncol.2020.1808
6. Natasya Naili MN, Hasnita CH, Shamim AK, *et al.* (2010) Chromosomal alterations in Malaysian patients with nasopharyngeal carcinoma analyzed by comparative genomic hybridization. *Cancer Genet Cytogenet,* ***203****(2): 309-12*. DOI: 10.1016/j.cancergencyto.2010.07.136
7. Smith ER, Wang J-Q, Yang D-H, Xu X-X (2022) Paclitaxel resistance related to nuclear envelope structural sturdiness. *Drug Resist Updat,* ***65****: 100881*. DOI: 10.1016/j.drup.2022.100881
8. West H, McCleod M, Hussein M, Morabito A, Rittmeyer A, Conter HJ, *et al*. (2019) Atezolizumab in combination with carboplatin plus nab-paclitaxel chemotherapy compared with chemotherapy alone as first-line treatment for metastatic non-squamous non-small-cell lung cancer (IMpower130): a multicentre, randomised, open-label, phase 3 trial. *Lancet Oncol,* ***20****(7): 924-937*. DOI: 10.1016/S1470-2045(19)30167-6
9. Yuan Y, Lee JS, Yost SE, *et al*. (2021) Phase II trial of neoadjuvant carboplatin and nab-paclitaxel in patients with triple-negative breast cancer. *Oncologist,* ***26****(3): e382-e393*. DOI: 10.1002/onco.1357
10. Parisi A, Palluzzi E, Cortellini A, *et al*. (2020) First-line carboplatin/nab-paclitaxel in advanced ovarian cancer patients, after hypersensitivity reaction to solvent-based taxanes: a single-institution experience. *Clin Transl Oncol,* ***22****(1): 158-162*. DOI: 10.1007/s12094-019-02122-x
11. Huang Y, Yan D, Wang M, *et al*. (2021) Clinicopathological factors affecting the prognosis of massive hemorrhage after radiotherapy for patients having nasopharyngeal carcinoma. *J Cancer Res Ther,* ***17****(5): 1219-1224*. DOI: 10.4103/jcrt.jcrt_586_21
12. Liu L, Hu L, Zeng Q, Peng D, Chen Z, Huang C, *et al*. (2021) Dynamic contrast-enhanced MRI of nasopharyngeal carcinoma: correlation of quantitative dynamic contrast-enhanced magnetic resonance imaging (DCE-MRI) parameters with hypoxia-inducible factor 1α expression and tumor grade/stage. *Ann Palliat Med,* ***10****(2): 2238-2253*. DOI: 10.21037/apm-21-303
13. Hengrui L (2023) An example of toxic medicine used in traditional Chinese medicine for cancer treatment. *J Tradit Chin Med,* ***43****(2): 209-210*. DOI: 10.19852/j.cnki.jtcm.2023.02.001
14. Kramer K, Pandit-Taskar N, Kushner BH, Zanzonico P, Humm JL, Tomlinson U, *et al*. (2022) Phase 1 study of intraventricular 131I-omburtamab targeting B7H3 (CD276)-expressing CNS malignancies. *J Hematol Oncol,* ***15****(1): 165*. DOI: 10.1186/s13045-022-01383-4
15. Baloche V, Ferrand FR, Makowska A, *et al.* (2020) Emerging therapeutic targets for nasopharyngeal carcinoma: opportunities and challenges. *Expert Opin Ther Targets,* ***24****(6): 545-558*. DOI: 10.1080/14728222.2020.1751820
16. Mai HQ, Chen QY, Chen D, *et al.* (2021) Toripalimab or placebo plus chemotherapy as first-line treatment in advanced nasopharyngeal carcinoma: a multicenter randomized phase 3 trial. *Nat Med,* ***27****(9): 1536-1543*. DOI: 10.1038/s41591-021-01444-0
17. Twu CW, Lin PJ, Tsou HH, *et al*. (2022) Maintenance metronomic chemotherapy for metastatic/recurrent nasopharyngeal carcinoma. *Head Neck,* ***44****(6): 1453-1461*. DOI: 10.1002/hed.27044
18. Li WZ, Lv X, Hu D, Lv SH, Liu GY, Liang H, *et al*. (2022) Effect of induction chemotherapy with paclitaxel, cisplatin, and capecitabine vs cisplatin and fluorouracil on failure-free survival for patients with stage IVA to IVB nasopharyngeal carcinoma: a multicenter phase 3 randomized clinical trial. *JAMA Oncol,* ***8****(5): 706-714*. DOI: 10.1001/jamaoncol.2022.0122
19. Takeshita N, Enokida T, Okano S, *et al*. (2022) Induction chemotherapy with paclitaxel, carboplatin and cetuximab for locoregionally advanced nasopharyngeal carcinoma: A single-center, retrospective study. *Front Oncol,* ***12****: 951387*. DOI: 10.3389/fonc.2022.951387
20. Luo DH, Li XY, Guo SS, *et al*. (2023) Paclitaxel liposome, cisplatin and 5-fluorouracil-based induction chemotherapy followed by de-escalated intensity-modulated radiotherapy with concurrent cisplatin in stage IVA-IVB childhood nasopharyngeal carcinoma in endemic area: a phase II, single-arm trial. *Lancet Reg Health West Pac,* ***40****: 100895*. DOI: 10.1016/j.lanwpc.2023.100895
21. Sharifi-Rad J, Quispe C, Patra JK, *et al*. (2021) Paclitaxel: Application in modern oncology and nanomedicine-based cancer therapy. *Oxid Med Cell Longev,* ***2021****: 3687700*. DOI: 10.1155/2021/3687700
22. Liu H and Li Y (2022) Potential roles of Cornichon family AMPA receptor auxiliary protein 4 (CNIH4) in head and neck squamous cell carcinoma. *Cancer Biomark,* ***35****(4): 439-450*. DOI: 10.3233/CBM-220143
23. Ke LR, Xia WX, Qiu WZ, *et al.* (2017) A phase II trial of induction NAB-paclitaxel and cisplatin followed by concurrent chemoradiotherapy in patients with locally advanced nasopharyngeal carcinoma. *Oral Oncol,* ***70****: 7-13*. DOI: 10.1016/j.oraloncology.2017.04.018
24. Thawani R, Gao L, Mohinani A, Tudorica A, Li X, Mitri Z, *et al*. (2022) Quantitative DCE-MRI prediction of breast cancer recurrence following neoadjuvant chemotherapy: a preliminary study. *BMC Med Imaging,* ***22****(1): 182*. DOI: 10.1186/s12880-022-00908-0
25. Militello C, Rundo L, Dimarco M, *et al*. (2022) 3D DCE-MRI radiomic analysis for malignant lesion prediction in breast cancer patients. *Acad Radiol,* ***29****(6): 830-40*. DOI: 10.1016/j.acra.2021.08.024
26. Filella X, Rodríguez-Garcia M, Fernández-Galán E (2022) Clinical usefulness of circulating tumor markers. *Clin Chem Lab Med,* ***61****(5): 895-905*. DOI: 10.1515/cclm-2022-1090
27. Jiang M, Chen P, Guo X, *et al*. (2023) Identification of EGFR mutation status in male patients with non-small-cell lung cancer: role of 18F-FDG PET/CT and serum tumor markers CYFRA21-1 and SCC-Ag. *EJNMMI Res,* ***13****(1): 27*. DOI: 10.1186/s13550-023-00976-5
28. Choi KH, Yu M, Jeong S, Lee JH (2020) Can serial evaluation of serum SCC-Ag-level predict tumor recurrence and patient survival in squamous-cell carcinoma of uterine cervix treated with definitive chemoradiotherapy? A multi-institutional analysis. *Int J Clin Oncol,* ***25****(7): 1405-1411*. DOI: 10.1007/s10147-020-01664-3
29. Gebhart P, Singer CF, Gschwantler-Kaulich D. (2023) CA125 Levels in BRCA mutation carriers - a retrospective single center cohort study. *BMC Cancer,* ***23****(1): 610*. DOI: 10.1186/s12885-023-11116-6
30. Li S, Pi G, Zeng Y, *et al*. (2022) Notoginsenoside R1 induces oxidative stress and modulates LPS induced immune microenvironment of nasopharyngeal carcinoma. *Int Immunopharmacol,* ***113****(Pt A): 109323*. DOI: 10.1016/j.intimp.2022.109323
31. Qiu W, Jiang J, Zhan Z, *et al*. (2022) Prognostic impact of pretreatment serum superoxide dismutase activity in patients with locoregionally advanced nasopharyngeal carcinoma. *Int J Biol Markers,* ***37****(1): 21-30*. DOI: 10.1177/17246008221075042
32. Gao H, Xie R, Huang R, *et al*. (2022) CIRBP regulates pancreatic cancer cell ferroptosis and growth by directly binding to p53. *J Immunol Res,* ***2022****: 2527210*. DOI: 10.1155/2022/2527210
33. Amina G, Hasnae D, Imane EA, *et al.* (2022) Assessment of lipid peroxidation status in the serum of Moroccan patients with nasopharyngeal carcinoma. *Contemp Oncol (Pozn),* ***26****(4): 253-258*. DOI: 10.5114/wo.2023.124498
34. Chen L, Hu CS, Chen XZ, *et al*. (2012) Concurrent chemoradiotherapy plus adjuvant chemotherapy versus concurrent chemoradiotherapy alone in patients with locoregionally advanced nasopharyngeal carcinoma: a phase 3 multicentre randomised controlled trial. *Lancet Oncol,* ***13****(2): 163-71*. DOI: 10.1016/S1470-2045(11)70320-5.

[Downloaded from mail.ijrr.com on 2025-12-22]

[DOI: 10.61186/ijrr.23.2.23]

[DOI: 10.61186/ijrr.23.2.23] [Downloaded from mail.ijrr.com on 2025-12-22]